Materials Research Proceedings 28 (2023) 987-1006 https://doi.org/10.21741/9781644902479-109

Electrically-assisted deep drawing of 5754 aluminium alloy sheet

DOBRAS Daniel[1,a *], ZIMNIAK Zbigniew[1,b] and ZWIERZCHOWSKI Maciej[1,c]

[1]Department of Metal Forming, Welding and Metrology, Wrocław University of Science and Technology, 7-9 Ignacego Łukasiewicza Street, 50-371 Wrocław, Poland

[a]daniel.dobras@pwr.edu.pl, [b]zbigniew.zimniak@pwr.edu.pl, [c]maciej.zwierzchowski@pwr.edu.pl

Keywords: Electrically-Assisted Forming, Aluminium Alloys, Deep Drawing

Abstract. The effect of current pulse application on the mechanical behaviour and plasticity of the 5754 aluminium alloy was studied. Tensile and deep drawing tests were conducted. The 5754 aluminium alloy in two different states of hardening was used: H111 and H22. The results show that the application of current pulses can significantly increase the plasticity of the examined alloys in the case of the tensile test. The dynamic recovery process is the main process responsible for the increase in plasticity of the material. However, in the case of the deep drawing process, it was observed that the increase in the material formability is low, and further studies are needed.

Introduction

Aluminium alloys have become very popular in the automotive industry owing to their good specific strength and corrosion resistance. However, the formability of many aluminium alloys at room temperature is low [1,2]. Warm and hot forming methods are applied in metal forming processes because they improve the formability of materials such as aluminium or magnesium alloys [3]. However, these methods have many drawbacks, such as increased adhesion of the die and decreased die strength and lubrication effectiveness [4].

Electrically-Assisted Forming (EAF) is proposed as an alternative method to the warm and hot forming methods. It is commonly known that the application of current pulses during plastic forming of metals can significantly increase their formability, reduce flow stress, and avoid or reduce some of the above-mentioned drawbacks [5–7]. Jeong et al. [8] showed that the application of current pulses during tension can increase the material elongation by over 200% in the case of the 5052-H32 aluminium alloy (AA) [9] and the as-extruded AZ91 magnesium alloy. Because this significant increase of the material plasticity during EAF processes cannot be explained only by the simple Joule heat law, many scientists have tried to explain this phenomenon [10]. There is still no unequivocal proof of existence of non-thermal effects such as the electroplastic effect [11], the magnetoplastic effect [12] or others [13]. The microscale Joule heat theory, more popular in the recent years, has been confirmed by the simulation [14], grain boundary melting [15] or such processes as dynamic recovery and recrystallization [8,16]. However, it does not explain all the observed phenomena [16]. Recently, it has been proved that the application of even low energy current pulses can lead to defect reconfiguration and a change in the dislocation pattern [17–19].

Many industrial metal forming processes have been supported by the application of current pulses. EAF processes such as wire drawing [20,21] or rolling [22,23] have been successfully realized. However, more difficult processes, in terms of EAF, such as deep drawing and press stamping, still need to be developed due to the unsatisfactory results. Only in the case of magnesium alloys the increase of plasticity has been meaningful [24,25]. In the electrically-assisted deep drawing processes, the following problems should still be overcome: excessive heat transfer from the sample to the dies, limited possibility of measuring the temperature or the need to apply higher currents [26–28].

Materials Research Proceedings 28 (2023) 987-1006 https://doi.org/10.21741/9781644902479-109

Materials and Methods

The tested material was the 5754 aluminium alloy, delivered in two different states of hardening: H111 and H22. The thickness of both as-received sheets was 1 mm. In the present work, two different electrically-assisted forming processes were conducted: the tensile test and the deep drawing test. The tensile samples with a gauge length of 75 mm and a gauge width of 12 mm were prepared by way of milling along the rolling direction of the sheet. The tensile tests were performed at a strain rate of 0.0025 s^{-1} until fracture using an INSTRON 3369 tensile machine.

The deep drawing tests were carried out at the punch speed of 0.4 mm/s until fracture using an Erichsen 142 Sheet Metal Testing Machine. The experimental study proved that a greater contact between the sample and the dies results in more heat transfer. Therefore, to avoid excessive heat transfer from the sample to the dies, the Erichsen machine was working in the sheet holder quick release (SHQR) mode. This means that, when the set draw depth is reached, the blank holder force is released, and the test continues until stopped. For the same reason, the dies were made of stainless steel because of its low thermal conductivity and high electrical resistance. Before the SHQR, the blank holder force was 35 and 40 kN, in the case of the H111 and the H22 state, respectively. A circular punch with a diameter of 30 mm and a radius of 4 mm as well as a matrix with a diameter of 33.5 mm and a radius of 4 mm were used in the deep drawing tests. A special sample, with experimentally fitted dimensions visible in Fig. 1, was used for the tests. The distance of 130 mm (Fig. 1) is the distance between the edges of the electrodes attached to the sample. The central, circular part of the sample with a radius of 32 mm was cut on the sides in order to obtain the highest current density. The dies were isolated from the machine. The sample mounted to the electrodes before the deep drawing process is visible in Fig. 2.

During all the tests, the electric pulses were generated by a self-constructed current pulse generator working at 2.52 V [29] and applied to the sample through copper electrodes attached to it. The applied current was pulsed with a pulse duration of t_d and a period of t_p, and its shape was created by the function generator device. The first pulse of electric current was applied after a time of t_p from the beginning of the tensile test, and from the moment of sheet holder force release in the case of deep drawing. An oscilloscope and a Rogowski coil were used to measure the current flowing through the samples. Each test was repeated three times. One side of the sample was sprayed with black paint, and its temperature was measured by a FLIR T440 infrared thermal imaging camera during the test.

The microstructural observations of the selected specimens were conducted with a VEGA3 TESCAN Scanning Electron Microscope (SEM) operating at 20 kV, and equipped with an Electron Backscattered Diffraction (EBSD) detector (Oxford Instruments). Mechanical grinding and electrolytic polishing using A2 Struers reagent were applied to prepare the specimen surfaces for the EBSD analysis. The applied step size was 0.2 µm. In the case of the non-EA specimen, the single-iteration grain dilation cleanup procedure was performed only one time and affected less than 4% of the measurement pixels.

Materials Research Proceedings 28 (2023) 987-1006 https://doi.org/10.21741/9781644902479-109

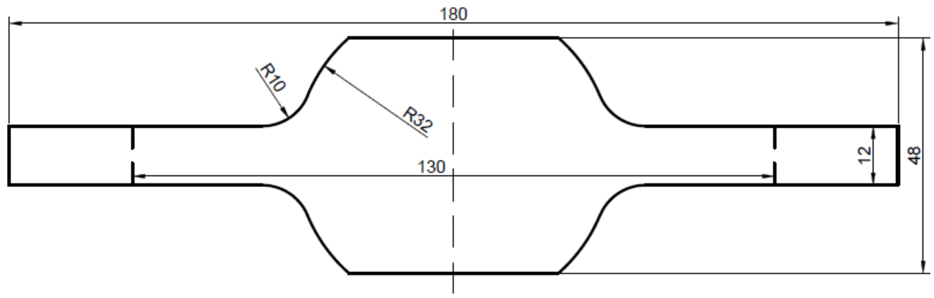

Fig. 1. The shape and dimensions (in mm) of the samples used in the deep drawing tests.

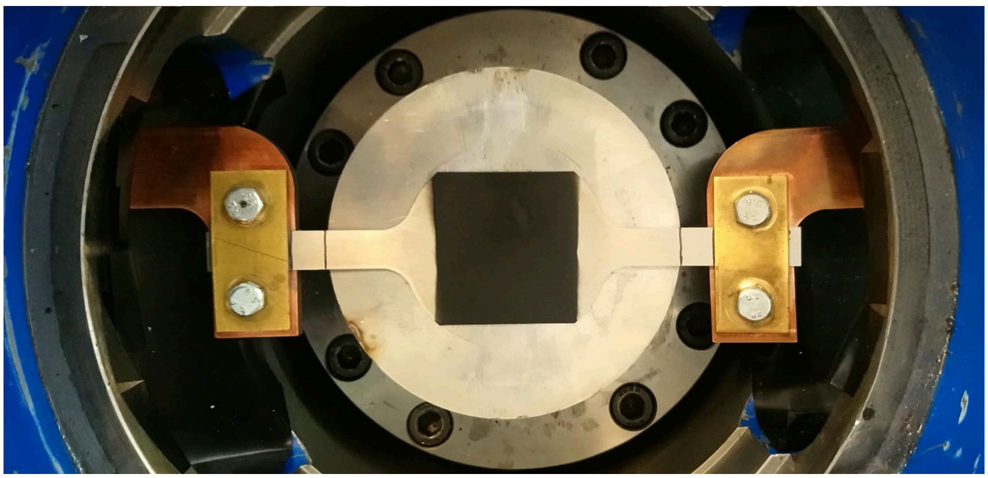

Fig. 2. The setup of the deep drawing sample before the process.

Results and Discussion

One of the most important current parameters in the EAF processes is the current density. Here, the nominal current density is defined as the current measured by the Rogowski coil divided by the cross-sectional area of the sample. The obtained values of the current density, depending on the applied process type and current parameters, are given in Table 1 and 2. Note that the current density in the case of deep drawing is about four times lower than in the case of the tensile test as a result of a four time higher width of the deep drawing samples and no possibility to increase the current. Therefore, as can be seen in Table 1 and 2, the pulses were applied more often in the case of deep drawing.

Table 1. Influence of current parameters on the current density for tensile test.

t_d / t_p [ms / s]	Current density [A/mm^2]	
	5754-H111	5754-H22
400 / 50	190	-
400 / 24	-	200

Table 2. Influence of current parameters on the current density for deep drawing test.

<table>
<tr><td>t_d / t_p [ms / s]</td><td colspan="2">Current density [A/mm^2]</td></tr>
<tr><td></td><td>5754-H111</td><td>5754-H22</td></tr>
<tr><td>400 / 2</td><td rowspan="4">45</td><td rowspan="4">45</td></tr>
<tr><td>400 / 1.2</td></tr>
<tr><td>500 / 2.5</td></tr>
<tr><td>500 / 1.5</td></tr>
</table>

Materials Research Proceedings 28 (2023) 987-1006 https://doi.org/10.21741/9781644902479-109

The engineering stress-strain curves of AA5754-H111 and AA5754-H22 with and without the current pulse application are shown in Fig. 3a-b. It is clearly seen that the application of the current pulses increase the material elongation. As can be seen, when the current pulse is applied, immediately, the engineering stress decreases and the temperature increases. The significant engineering stress drop is, among others, correlated with the sample's thermal expansion. However, before the next pulse application, the temperature drops almost to the room value. In the case of the annealed state (H111), the average value of engineering strain increased from 22.86 to 32.73% (increase to about 143% of the basic value). However, in the case of the hardened alloy (H22), the

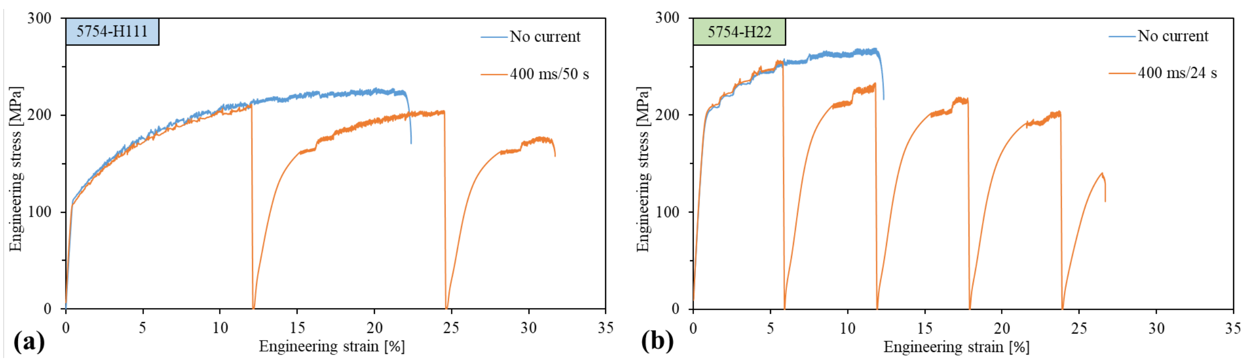

Fig. 3. Engineering stress-strain curves of 5754 AA in the a) H111 and b) H22 state with and without current application.

average value of engineering strain increased from 12.27 to 27.13% (increase to about 221% of the basic value). It is worth mentioning that the ratio of t_d/t_p was 1/60 in the case of the hardened alloy, and it was the best ratio in terms of increasing the material elongation. Nevertheless, in the case of the annealed alloy the similar increase the material elongation occurred for a wide range of t_d/t_p ratios. The average values of the maximal registered temperatures during tensile tests were 364 and 390ºC, for AA5754-H111 and AA5754-H22, respectively. However, in both cases, the average temperature during all the tensile tests was under 200ºC, which is generally a lower temperature than the warm forming temperature for these alloys.

Fig. 4a-b present the deep drawing force-displacement curves of the 5754 aluminium alloy. The force represents the force at the punch in the deep drawing process and the displacement is the displacement of the punch, which corresponds with the depth of the drawpiece. The SHQR took places 5.4 and 3.4 mm from the beginning of the tests for the annealed and the hardened alloy, respectively. The above-mentioned values were experimentally designated, and the obvious decrease of the force corresponds to the SHQR moment. Unlike the tensile tests, in the deep drawing tests, the application of the current pulses did not lead to a significant increase of the drawpieces' heights. Only in one case, the height of the drawpiece increased noticeably, when the 500 ms/1.5 s current parameters were applied to the 5754-H111 aluminium alloy (Fig. 4a). In this case, the displacement at the punch increased about 8% in comparison with the baseline value (Fig. 5a), but in other cases, the displacement increase or decrease were not greater than 2% (Fig. 5a-b). The average values of the maximal registered temperatures during the deep drawing tests, for the different current parameters, are presented in Fig. 6a-b. The temperature did not exceed 80ºC in any case. A picture of an example drawpiece of 5754-H22 AA is visible in Fig. 7. A characteristic fracture is visible on the top edge of the drawpiece.

Materials Research Proceedings 28 (2023) 987-1006 https://doi.org/10.21741/9781644902479-109

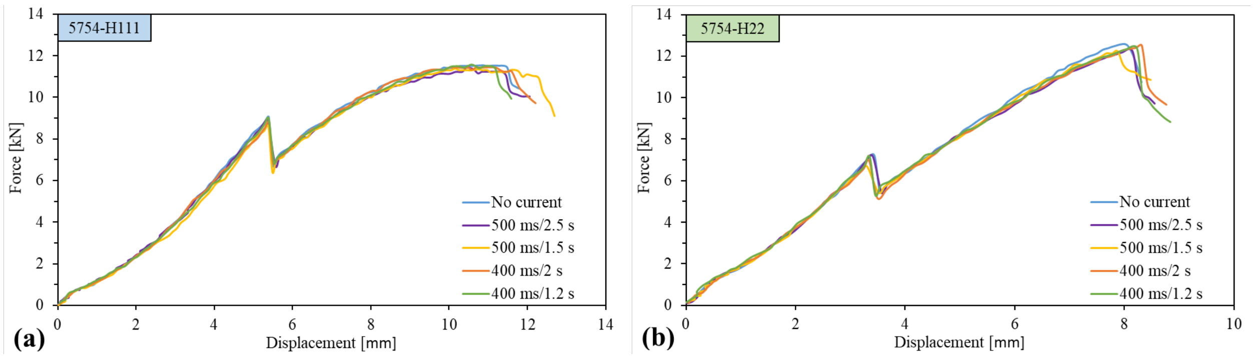

Fig. 4. Deep drawing force-displacement curves of 5754 AA in the a) H111 and b) H22 state with and without current application.

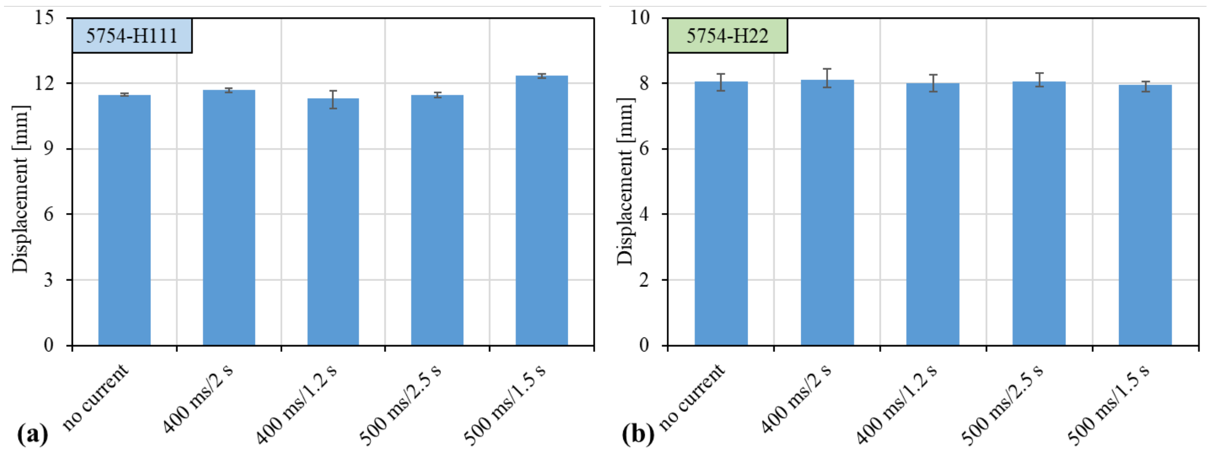

Fig. 5. Influence of the current parameters on the height of the drawpieces of 5754 AA in the a) H111 and b) H22 state.

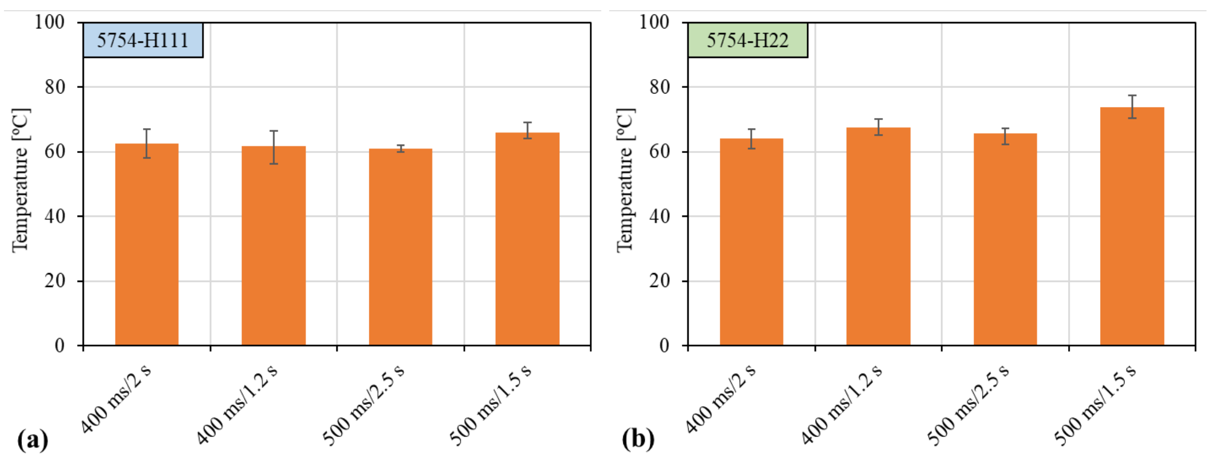

Fig. 6. Influence of the current parameters on the maximal temperature of the drawpieces of 5754 AA in the a) H111 and b) H22 state.

Fig. 7. The example drawpiece of 5754-H22 AA.

Even if the application of the current pulses leads to a significant increase of the material elongation in the tensile tests, it is difficult to reproduce the same conditions and results in the deep drawing process. The current density present during deep drawing is about four times lower than in the case of a tensile, and it is the main reason for the insignificant increase of the material formability. Low current density resulted in low temperature of the tested samples, which did not increase even when the pulses were applied more often. Finally, the dynamic recovery and recrystallization processes cannot take place and increase the material plasticity when the temperature is too low. The solution of the above-mentioned problems will be the application of a large high-current pulse generator, with the possibility of applying high currents. However, this solution increases the process costs and makes it more difficult, yet it will be necessary in potential industrial applications.

The highest increase of the material plasticity, owing to the pulsed current application, occurred in the case of the 5754-H22 AA tensile sample. Therefore, the specimens from the 5754-H22 AA tensile tests were selected for the microstructural analysis. In order to better analyze the effect of the current pulses on the structural changes, two additional tests were conducted. In the first case, the EA tensile test was immediately stopped after the fourth pulse application (Fig. 3b). It happened at 90% elongation of the EA tensile sample. In the second case, the non-EA tensile sample was stretched to a 90% value of its initial elongation and then the test was also stopped. The specimens for the microstructural analysis were cut from the middle of the above-mentioned tensile samples.

The Inverse Pole Figure (IPF) maps of the non-EA and EA specimens are presented in Fig. 8 a) and b), respectively. Due to the high deformation of the crystal lattice, the initial Hit Rate value of the non-EA specimen was only about 60%, which is typical for highly deformed materials. Although the EA specimen was deformed to a greater extent (about two times greater elongation, Fig. 3b), the obtained Hit Rate in this case was more than 80%. It means that the crystal lattice deformation is lower than for the specimen without the current application. If the material has been deformed more, but its lattice is less deformed, then the application of the current pulses and the increase of temperature resulting from it lead to a lattice structure rebuild. The IPF maps represent the above-mentioned case.

Many small grains are visible (Fig. 8b) at grain boundaries of the big and medium size grains in the case of specimen with the pulsed current application. It could mean that the dynamic recrystallization process occurred, especially because, for a while, the temperature during the EA tensile tests reached the value of $0.6T_m$, where T_m is the homologous temperature of aluminium. However, a more detailed analysis is needed to verify this hypothesis.

To analyze the recrystallization process, the Grain Orientation Spread (GOS) parameter was used. Generally, it is assumed that the GOS parameter for recrystallized grains is less than 1.5-2 º. However, this threshold value in the literature ranges from 1 to 3 º [9,30]. In this study the

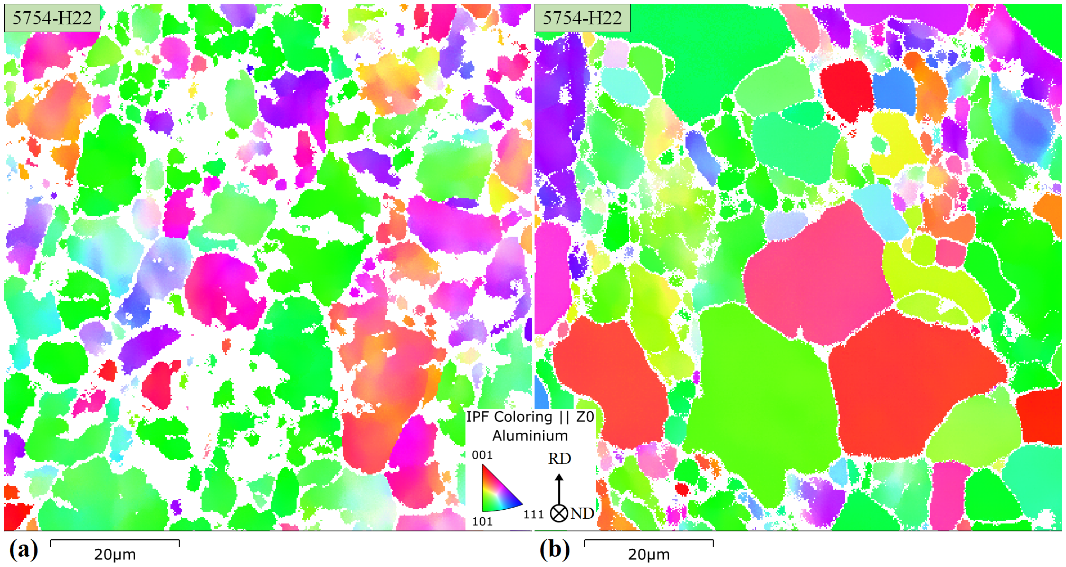

Fig. 8. IPF maps of 5754-H22 AA from a stopped a) non-EA and b) EA tensile test.

recrystallized grains are defined by the GOS less than 1.5 º. The GOS map of non-pulsed specimen is presented in Fig. 9a. It is clearly seen that the most grains are characterized by the GOS higher than 2 º, and only about 13% indexed pixels - by the GOS less than 1.5 º. It could mean that these grains with lower GOS parameter were not deformed or deformed in a small range. Completely different results are shown by the GOS map of the pulsed specimen (Fig. 9b). The effect of temperature resulted in a significant increase in the surface of grains, with the GOS less than 1.5 º. It this case about 62% indexed pixels is characterized by the GOS less than 1.5 º. However, mainly the large grains take small values of the GOS parameter. Therefore, it can be concluded that the intense dynamic recovery process occurred in these large grains. This recovery process led to a structure rebuild of the crystal lattice in grains and thus to the low GOS parameter. On the other hand, many small grains with the GOS less than 1.5 º are visible at grain boundaries of the bigger grains. It could mean that the dynamic recrystallization process started in these places, however, a more detailed analysis using transmission electron microscopy should be performed to prove it.

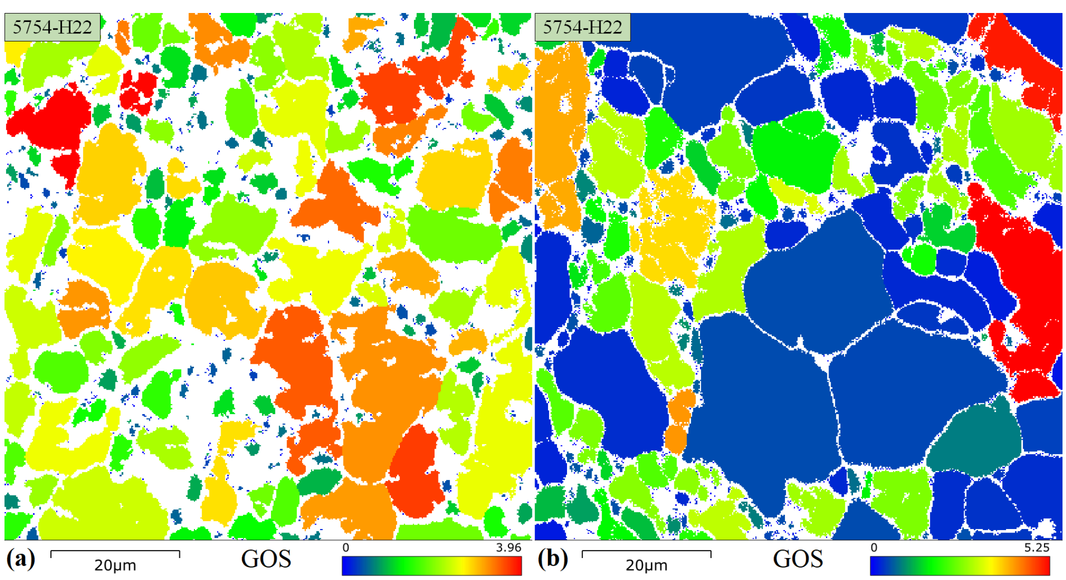

Fig. 9. GOS maps of 5754-H22 AA from a stopped a) non-EA and b) EA tensile test.

Summary

In the present work, electrically-assisted tensile tests and deep drawing processes of the 5754 aluminium alloy in different states of hardening were carried out. The main conclusions are:

1. The application of current pulses can lead to a significant increase of the material elongation in the tensile test, especially in the case of the H22 state.
2. The EBSD analysis proved that the intense dynamic recovery is the main factor responsible for the structure rebuild of the crystal lattice and thus the increase of the material plasticity.
3. The application of the sheet holder quick release mode, new in terms of electrically-assisted forming, can lead to a decrease of the excessive heat transfer from sample to the dies.
4. The application of the current pulses did not lead to a significant increase of the material formability in the case of the deep drawing process. The main difficulties in effective implementation of the electrically-assisted deep drawing processes are the necessity of the application of high currents and an excessive heat transfer from the sample to the stamping dies.

References

[1] Z. Gronostajski, K. Jaśkiewicz, P. Kaczyński, M. Skwarski, S. Polak, J. Krawczyk, W. Chorzępa, P. Trzpis, W-Temper forming of B-pillar from 7075 aluminum alloy, CIRP Ann. 71 (2022) 221–224. https://doi.org/10.1016/j.cirp.2022.03.019

[2] H. Deng, Y. Mao, G. Li, X. Zhang, J. Cui, AA5052 failure prediction of electromagnetic flanging process using a combined fracture model, Arch. Civ. Mech. Eng. 22 (2022) 1-17. https://doi.org/10.1007/s43452-022-00390-z

[3] S. Toros, F. Ozturk, I. Kacar, Review of warm forming of aluminum-magnesium alloys, J. Mater. Process. Technol. 207 (2008) 1–12. https://doi.org/10.1016/j.jmatprotec.2008.03.057

[4] W.A. Salandro, J.T. Roth, Formation of 5052 aluminum channels using Electrically-Assisted Manufacturing (EAM), Proc. ASME Int. Manuf. Sci. Eng. Conf. 2009, MSEC2009. 2 (2009) 599-608. https://doi.org/10.1115/MSEC2009-84117

[5] H.R. Dong, X.Q. Li, Y. Li, Y.H. Wang, H.B. Wang, X.Y. Peng, D.S. Li, A review of electrically assisted heat treatment and forming of aluminum alloy sheet, Int. J. Adv. Manuf. Technol. 120 (2022) 7079–7099. https://doi.org/10.1007/s00170-022-08996-6

[6] E. Simonetto, S. Bruschi, A. Ghiotti, Electroplastic effect on AA1050 plastic flow behavior in H24 tempered and fully annealed conditions, Procedia Manuf. 34 (2019) 83-89. https://doi.org/10.1016/j.promfg.2019.06.124

[7] B.J. Ruszkiewicz, T. Grimm, I. Ragai, L. Mears, J.T. Roth, A Review of Electrically-Assisted Manufacturing with Emphasis on Modeling and Understanding of the Electroplastic Effect, J. Manuf. Sci. Eng. Trans. ASME. 139 (2017) 1–15. https://doi.org/10.1115/1.4036716

[8] J.H. Roh, J.J. Seo, S.T. Hong, M.J. Kim, H.N. Han, J.T. Roth, The mechanical behavior of 5052-H32 aluminum alloys under a pulsed electric current, Int. J. Plast. 58 (2014) 84-99. https://doi.org/10.1016/j.ijplas.2014.02.002

[9] H.J. Jeong, M.J. Kim, J.W. Park, C.D. Yim, J.J. Kim, O.D. Kwon, P.P. Madakashira, H.N. Han, Effect of pulsed electric current on dissolution of Mg17Al12 phases in as-extruded AZ91 magnesium alloy, Mater. Sci. Eng. A. 684 (2017) 668-676. https://doi.org/10.1016/j.msea.2016.12.103

[10] N.K. Dimitrov, Y. Liu, M.F. Horstemeyer, Electroplasticity: A review of mechanisms in electro-mechanical coupling of ductile metals, Mech. Adv. Mater. Struct. 0 (2020) 1-12. https://doi.org/10.1080/15376494.2020.1789925

[11] K. Okazaki, M. Kagawa, H. Conrad, A study of the electroplastic effect in metals, Scr. Metall. 12 (1978) 1063-1068. https://doi.org/10.1016/0036-9748(78)90026-1

[12] M.I. Molotskii, Theoretical basis for electro- and magnetoplasticity, Mater. Sci. Eng. A. 287 (2000) 248-258. https://doi.org/10.1016/s0921-5093(00)00782-6

[13] B.J. Ruszkiewicz, L. Mears, J.T. Roth, Investigation of Heterogeneous Joule Heating as the Explanation for the Transient Electroplastic Stress Drop in Pulsed Tension of 7075-T6 Aluminum, J. Manuf. Sci. Eng. Trans. ASME. 140 (2018) 1–11. https://doi.org/10.1115/1.4040349
[14] J. Zhao, G.X. Wang, Y. Dong, C. Ye, Multiscale modeling of localized resistive heating in nanocrystalline metals subjected to electropulsing, J. Appl. Phys. 122 (2017). https://doi.org/10.1063/1.4998938
[15] R. Fan, J. Magargee, P. Hu, J. Cao, Influence of grain size and grain boundaries on the thermal and mechanical behavior of 70/30 brass under electrically-assisted deformation, Mater. Sci. Eng. A. 574 (2013) 218–225. https://doi.org/10.1016/j.msea.2013.02.066
[16] M.J. Kim, S. Yoon, S. Park, H.J. Jeong, J.W. Park, K. Kim, J. Jo, T. Heo, S.T. Hong, S.H. Cho, Y.K. Kwon, I.S. Choi, M. Kim, H.N. Han, Elucidating the origin of electroplasticity in metallic materials, Appl. Mater. Today. 21 (2020) 100874. https://doi.org/10.1016/j.apmt.2020.100874
[17] S. Zhao, R. Zhang, Y. Chong, X. Li, A. Abu-Odeh, E. Rothchild, D.C. Chrzan, M. Asta, J.W. Morris, A.M. Minor, Defect reconfiguration in a Ti–Al alloy via electroplasticity, Nat. Mater. 20 (2021) 468-472. https://doi.org/10.1038/s41563-020-00817-z
[18] X. Li, J. Turner, K. Bustillo, A.M. Minor, In situ transmission electron microscopy investigation of electroplasticity in single crystal nickel, Acta Mater. 223 (2022) 117461. https://doi.org/10.1016/j.actamat.2021.117461
[19] X. Zhang, H. Li, M. Zhan, Z. Zheng, J. Gao, G. Shao, Electron force-induced dislocations annihilation and regeneration of a superalloy through electrical in-situ transmission electron microscopy observations, J. Mater. Sci. Technol. 36 (2020) 79-83. https://doi.org/10.1016/j.jmst.2019.08.008
[20] Z. Zimniak, G. Radkiewicz, The electroplastic effect in the cold-drawing of copper wires for the automotive industry, Arch. Civ. Mech. Eng. 8 (2008) 173–179. https://doi.org/10.1016/S1644-9665(12)60204-0
[21] G. Tang, J. Zhang, M. Zheng, J. Zhang, W. Fang, Q. Li, Experimental study of electroplastic effect on stainless steel wire 304L, Mater. Sci. Eng. A. 281 (2000) 263-267. https://doi.org/10.1016/s0921-5093(99)00708-x
[22] Z. Xu, G. Tang, S. Tian, F. Ding, H. Tian, Research of electroplastic rolling of AZ31 Mg alloy strip, J. Mater. Process. Technol. 182 (2007) 128-133. https://doi.org/10.1016/j.jmatprotec.2006.07.019
[23] H.D. Nguyen-Tran, H.S. Oh, S.T. Hong, H.N. Han, J. Cao, S.H. Ahn, D.M. Chun, A review of electrically-assisted manufacturing, Int. J. Precis. Eng. Manuf. - Green Technol. 2 (2015) 365-376. https://doi.org/10.1007/s40684-015-0045-4
[24] H. Xie, X. Dong, Z. Ai, Q. Wang, F. Peng, K. Liu, F. Chen, J. Wang, Experimental investigation on electrically assisted cylindrical deep drawing of AZ31B magnesium alloy sheet, Int. J. Adv. Manuf. Technol. 86 (2016) 1063–1069. https://doi.org/10.1007/s00170-015-8246-0
[25] Z. Lv, Y. Zhou, L. Zhan, Z. Zang, B. Zhou, S. Qin, Electrically assisted deep drawing on high-strength steel sheet, Int. J. Adv. Manuf. Technol. 112 (2021) 763-773. https://doi.org/10.1007/s00170-020-06335-1
[26] G.F. Wang, B. Wang, S.S. Jang, K.F. Zhang, Pulse current auxiliary thermal deep drawing of SiCp/2024Al composite sheet with poor formability, J. Mater. Eng. Perform. 21 (2012) 2062-2066. https://doi.org/10.1007/s11665-012-0165-8
[27] H.G. Park, B.S. Kang, J. Kim, Numerical modeling and experimental verification for high-speed forming of Al5052 with single current pulse, Metals 9 (2019). https://doi.org/10.3390/met9121311

[28] Y. Zhao, L. Peng, X. Lai, Influence of the electric pulse on springback during stretch U-bending of Ti6Al4V titanium alloy sheets, J. Mater. Process. Technol. 261 (2018) 12–23. https://doi.org/10.1016/j.jmatprotec.2018.05.030
[29] G. Lesiuk, Z. Zimniak, W. Wiśniewski, J.A.F.O. Correia, Fatigue lifetime improvement in AISI 304 stainless steel due to high-density electropulsing, Procedia Struct. Integr. 5 (2017) 928–934. https://doi.org/10.1016/j.prostr.2017.07.118
[30] M.H. Alvi, S. Cheong, H. Weiland, A.D. Rollett, Recrystallization and texture development in hot rolled 1050 aluminum, Mater. Sci. Forum. 467–470 (2004) 357–362. https://doi.org/10.4028/www.scientific.net/msf.467-470.357